Low-Cost Aacvd As The Proven Method to Fabricate Carbon Solar Cell

Nurfadzilah Ahmad[1], Habibah Zulkefle[2], Puteri Sarah Mohamad Saad[2], Sivaraju S. S[3], Nurdiyana Borhan[4], Wan Abd Al-Qadr Imad Wan Mohtar[5]

[1]Solar Research Institute (SRI), Universiti Teknologi MARA (UiTM) Shah Alam, Selangor, [2]School of Electrical Engineering, College of Engineering, Universiti Teknologi MARA (UiTM) Shah Alam, Selangor, [3]RVS College of Engineering and Technology, Coimbatore, Tamil Nadu, India, [4]Davex (Malaysia) Sdn. Bhd., Subang Jaya, Selangor, [5] Functional Omics and Bioprocess Development Laboratory, Institute of Biological Sciences, Faculty of Science, Universiti Malaya, 50603, Kuala Lumpur, Malaysia

Abstract
To deposit amorphous carbon (a-C) thin films for carbon-based solar cell applications, a novel self-prepared Aerosol-Assisted Chemical Vapour Deposition (AACVD) system was created. At deposition temperatures of 600°C and 650°C, nitrogen doping was applied to a-C thin films. Using the solar simulator system in low-light conditions, the samples demonstrated the photoresponse characteristic for electrical measurements.The nanostructured sized a-C:N (100nm) is represented by FESEM pictures, and the EDX spectrum confirms the presence of N content in the N doped a-C. When the a-C:N was coated on a p-Si substrate, the solar cell efficiency was 0.001648% at 650°C and 0.000124% at 600°C. The presence of rectifying curves at the a-C:N/p-Si junction implies hetero-junction behaviour between the p-n structure and hence demonstrates successful N doping of a-C utilising the AACVD process.
Keywords: Nitrogen Doping, AACVD, Amorphous Carbon, Carbon-based Solar Cell.

Introduction
Amorphous carbon (a-C) is an appealing material because of its low cost, ease of mass production, and semiconductor properties. The a-C, on the other hand, has a tuneable band gap that may be obtained by adjusting the sp2/sp3 ratio within the a-C (Omer et al., 2005; Robertson, 2002a). Various applications of a-C were researched, including protective and anti-reflective coatings for solar cells. However, the use and application of a-C as n-type carbon/p-type silicon or p-type carbon/n-type silicon to produce heterojunction devices via doping approach has recently expanded. Boron (B) or any other metal element is the most commonly utilised dopant for obtaining p-type a-C (Sitch et al., 1998). Nitrogen (N) is the most commonly employed dopant in the production of n-type a-C. Amorphous carbon doped with nitrogen (n-C: N) has been reported as a conductive material for electrical examination. A low background current, a large potential window, and inertness in chemically harsh settings are

only a few of the benefits (Zeng et al., 2005). Nitrogen (N) integrated a-C exhibits improved electrical conductivity and photoconductivity, both of which are relevant in solar cell applications (Liu et al., 2007). In this study, we will use an Aerosol-assisted CVD (AACVD) method to prepare Nitrogen doped amorphous carbon (n-C: N). Camphor oil was employed as the carbon precursor, and the in situ doping procedure was carried out with the assistance of N gas as the dopant source. The AACVD system was a modified standard CVD system that had been utilised for a long time to generate a-C thin films. However, traditional CVD had significant limitations, including the inability to choose and deliver multicomponent products due to a lack of a suitable volatile precursor and the difficulties in managing the deposition stoichiometry (Hou & Choy, 2006). To address the stated shortcomings, the standard CVD method was self-modified into aerosol-assisted CVD (AACVD). The AACVD technique involves the transformation of a liquid precursor into vapour, and the vaporised aerosol droplets are carried towards the heated substrate with the help of a carrier gas (inert gas). Other researchers used an AACVD approach to synthesise ZnO (Nolan et al., 2011) due to the low cost of the technology and the good characteristics of the thin films generated.

Methodology

The following is how the experimental details went. First, 2cm x 2cm glass substrates and 1.5cm x 1.5cm p-type (100) Si wafers were cleaned for 10 minutes each in ultrasonic baths of acetone, methanol, and deionized (DI) water. The goal of cleaning the substrates in the correct order is to promote a-C:N thin film adhesion to these substrates. The p-type Si wafers were also etched with 10% HF to remove the oxide layer on the substrate surfaces. Second, using a self-modified AACVD technique, the a-C:N thin films were deposited independently on p-type (100) Si wafers and glass substrates. The schematic diagram of the AACVD system, which was a combination of conventional CVD and spray pyrolysis, was shown in Fig. 1. The AACVD system employs a dual furnace system with a quartz tube as the deposition medium. The AACVD system began with a gas cylinder that transported vaporised camphor oil from the aerosol-assisted container to the second CVD furnace where deposition took place. Because the deposition and doping processes occurred concurrently, the doping process was characterised as in-situ doping. The reaction furnace was purged with N gas prior to deposition to maintain cleanliness, and the substrate temperature was 600oC and 650oC throughout deposition. The dopant and carrier gas, N, was kept at a constant flow rate of 7 standard cubic centimetres per minute (sccm). The deposition duration was set to 30 minutes.

The a-C thin films' properties were measured as follows. To acquire the ohmic contact characteristic of the a-C thin films, the electrical properties were characterised using a current-voltage Solar Simulator system. The UV-Vis-NIR spectroscope was used to characterise the transmittance and absorption behaviour, and the FESEM pictures were used to characterise the microstructure and chemical composition of the a-C. The J-V characteristic was also examined using the solar simulator system to see whether the a-C could be employed as a solar cell. Prior to characterization, the a-C:N and p-Si contacts were created by sputtering with 60nm gold (Au). Notably, only the J-V measurement was performed on a-C:N deposited on p-Si, whereas the other measurements were performed on a-C:N deposited on glass substrates.
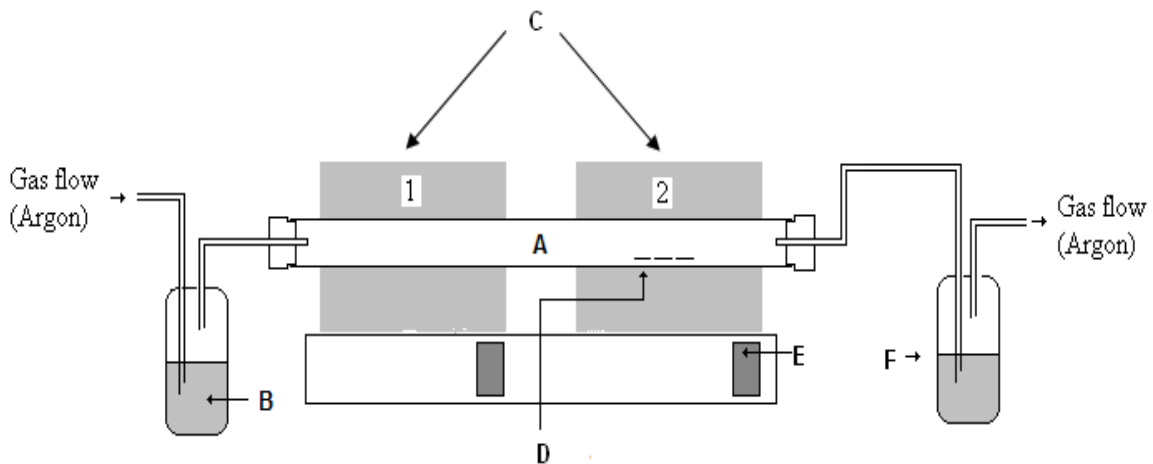
Fig. 1: AACVD using Camphor Oil as the precursor (A) Quartz tube (B) Camphor oil (C) Double furnace setup (D) Substrate (E) Temperature controller (F) Water bubbling system.

Results and Discussion

The electrical characteristics of a-C:N were measured using the Bukoh Keiki CEP2000 solar simulator system, and an ohmic graph was generated for a-C:N deposited at 600°C and 650°C, respectively. The supply voltage was set between -10 and 10 volts. The counter electrode was made of gold (Au) and had a thickness of 60nm. When nitrogen was utilised as the dopant/carrier gas, the current obtained for a-C: N was 10-5 A at 600°C and 10-2 A at 650°C. The greater the slope, the lower the resistance value. The resistivity (ρ) and conductivity (σ) values were estimated from the resistance value using equations (1) and (2), where R is the resistance acquired from the I-V curve, w is the electrode width, t is the thickness of the a-C thin film, and L is the electrode length.

$$\rho = \left(\frac{V}{I}\right)\left(\frac{wt}{L}\right) \quad \text{in unit } \Omega.\text{cm} \qquad (1)$$

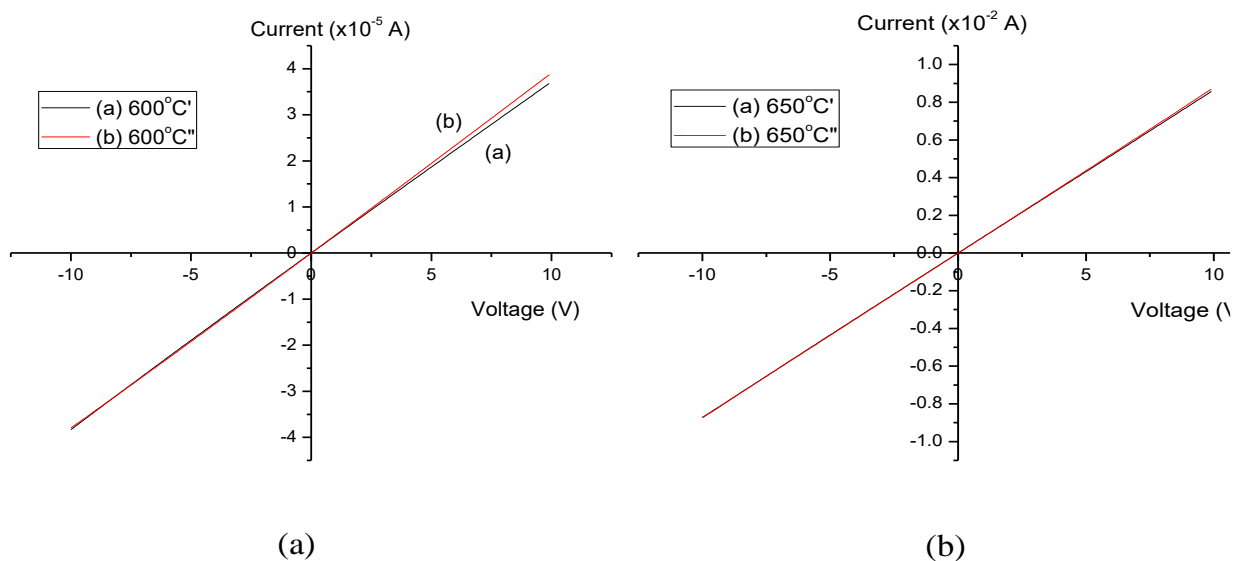$$\sigma = \frac{1}{\rho} \quad \text{in unit S.cm}^{-1} \qquad (2)$$

(a)

(b)

Fig.2. Current-voltage graph for a-C: N deposited at (a) 600°C and (b) 650°C.

The conductivity (σ) was computed and found to be 0.25 Scm-1 at 600°C and 38.70 Scm-1 at 650°C. Under low illumination, the value increased slightly to 0.26 Scm-1 and 38.99 Scm-1. The increase in conductivity when the sample was illuminated illustrates the photoresponse behaviour of the thin films. The photoresponse behaviour is critical for the material to be employed in carbon-based solar cell applications since it indicates the material's reaction to sunlight. As a result of the photoresponse property of a-C:N, it is clear that the a-C:N has a great potential for usage in carbon-based solar cell applications. The current flow in the external circuit is generated by electron-hole pairs separated by the electric field between the electrodes due to light absorption. Current flow is caused by photoexcited carriers drifting before recombination (Suemasu et al., 2011). Theoretically, density changes caused by crystal defects such as vacancies, grain boundaries, and film surfaces affect electrical characteristics since they are directly related to carrier concentration and mobility of electrons at different thicknesses of thin films (Huang & Meng, 2007).

Because nitrogen gas can shift the conductivity of pure a-C from p-type to n-type, samples deposited with nitrogen gas as the dopant/carrier gas exhibit higher conductivity. Successful doping is considered to reduce defects since the spin density gap decreases with nitrogen addition (Rusop et al., 2006). Aside from that, nitrogen addition has been shown to reduce compressive stress and enhance conductivity (Adhikari et al., 2006, 2008; A. Liu et al., 2008;Yap et al., 2009). As a result, nitrogen doped a-C: N has a greater conductivity.
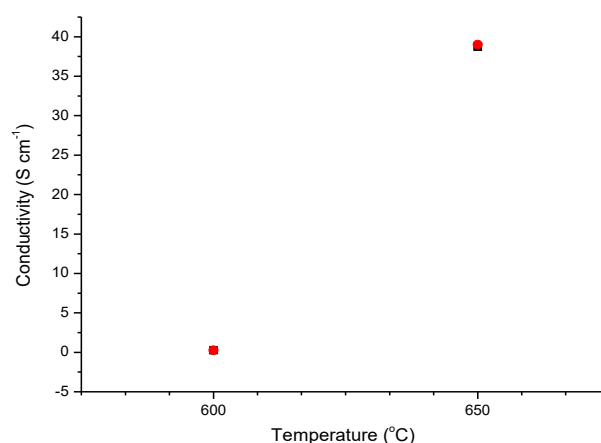

Fig.3. Conductivity for a-C: N deposited at 600°C and 650°C.

The linear graph generated for the complete sample, as shown in Fig. 2, indicates the ohmic contact characteristics. The linear graph shifts upwards as deposition time increases from 15 minutes to 45 minutes, indicating low electrical resistance of the sample; nevertheless, the linear graphs change downwards at 60 and 75 minutes. The I-V measurement, however, shows that all of the samples with low-resistive linear current-voltage have good ohmic contact. These I-V measurements demonstrate that the graphitic behaviour within the a-C can act as conductive pathways for electron transport (Robertson, 2002b). The electrical conductivity was plotted as shown in Fig. 3 and the sample with the sharpest I-V slope (45 minutes) had the greatest. As a result, we may conclude that 45 minutes is the optimal deposition period for producing the a-C thin film. The a-C characteristic was evaluated in the dark and under illumination conditions AM 1.5 (100 mW/cm2, 25°C). The thickness of the thin films was measured using a surface profiler, and it was discovered that as deposition time grew (15 minutes to 75 minutes), so did the thickness (30-90 nm).

When a-C is exposed to darkness, all samples had lower conductivity values than when exposed to light. The in dark conductivity (d) of a-C deposited at 15 minutes was 3.3 x 10-4 Scm-1 and subsequently increased to 6.4 x 10-4 Scm-1 when the deposition period was increased to 30 minutes. At 45 minutes, the value skyrockets to 21 x 10-4 Scm-1. However, as the deposition duration increases to 60 and 75 minutes, the value reduces to 5.5 x 10-4 Scm-1 and 2.6 x 10-4 Scm-1, respectively. Karoui et al. (Hauser, 1977) reported a similar value. This conductivity trend is strongly related to the a-C thin films' carrier concentration and mobility (Robertson & Davis, 1995). The carrier mobility and concentration increase as the thickness increases (Singh et al., 2004), which explains the increase in conductivity from 15 to 45 minutes. However, the decreased conductivity values at 60 and 75 minutes may be due to structural defects in the thin films at higher deposition times. A-C conductivity is also influenced by the existence of * (sp2 graphitic bonding) and * (sp2 and sp3 diamond bonding). As the strength of the * region increases, so does the encouragement of sp2 bonding as graphitic order increases (Belaidi et al., 2003).

Samples a-C showed the same conductivity trend, albeit with a higher value, under AM 1.5 illumination (100 mW/cm2, 25°C). The under illumination conductivity (i) value begins at 3.7 x 10-4 Scm-1 for 15 minutes, gradually increases to 6.5 x 10-4 Scm-1 for 30 minutes, and sharply increases at 45 minutes (22 x 10-4 Scm-1). The upward movement of d to i represents the a-C photo response (Valentini et al., 2001). When lighted, the electron-hole pairs separated by the electric field between the electrodes from light absorption produce current flow. Current flow is caused by photoexcited carriers drifting before recombination. The conductivity ratio of under illumination to in darkness is shown in Table 1.
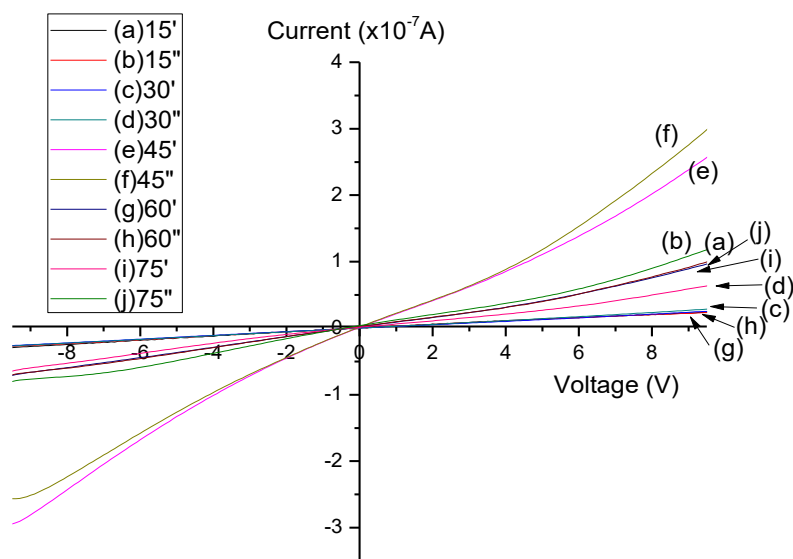

Fig 2: I-V graph for a-C thin films deposited at different deposition time.
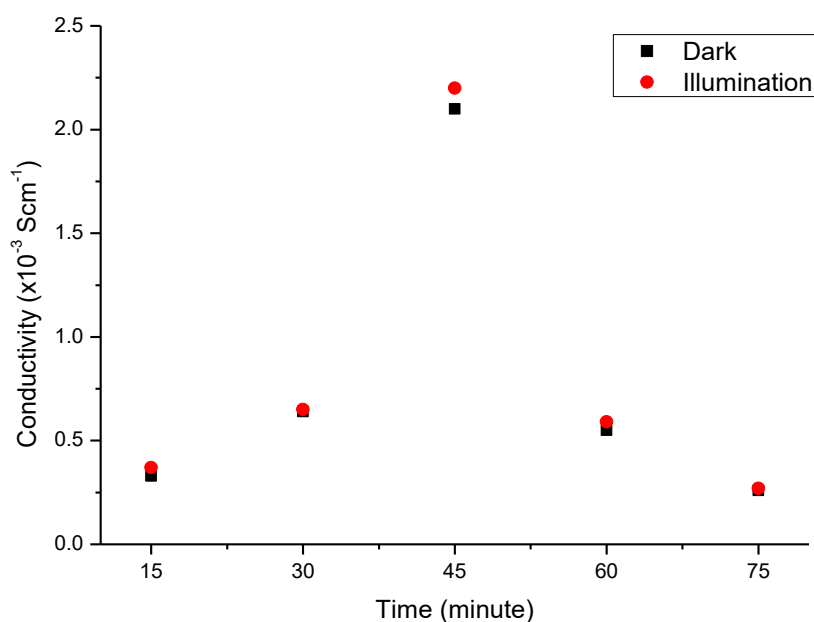("indicates the I-V graph under illumination condition).

Fig. 3: Conductivity graph for a-C thin films deposited at different deposition time.

Table 1
*Details on the conductivity value for a-C thin films deposited at different deposition time.*

Deposition Time	Conductivity ($\times 10^{-4}$ S cm^{-1})		σ_i/σ_d
	Under illumination	In dark	
15	3.7	3.3	1.12
30	6.5	6.4	1.01
45	22.0	21.0	1.05
60	5.9	5.5	1.07
75	2.7	2.6	1.04

Figure 7 depicts the results of a-C:N imaging using a Field Emission Scanning Electron Microscope (FESEM) at 100k X magnification and 10kV electron high tension (EHT). The average grain size for both samples was reported to be modest, around 4080nm, implying that the a-C thin film structure is nanostructured (less than 100nm). The sample displays a cloud-like image of a-C:N with no discernible shapes. The image was regarded successful, however, because the FESEM image for pure a-C and a-C:N was rarely recorded. The nanostructured material has some promising advantages for the a-C solar cell application, such as the optical absorption path is much larger (Singh et al., 2004), the absorber layer is thin, so the light generated electrons and holes only have to travel over a much shorter path, and thus recombination losses are greatly reduced (Belaidi et al., 2003). and the energy band can be modified by modifying the size of nanoparticles, allowing for more absorber layer designs in solar cells [(Singh et al., 2004). Nonetheless, successful nitrogen doping was validated by the energy dispersive X-ray analysis (EDX) spectrum data, which revealed the presence of the nitrogen (N) element in the a-C: N sample. As a result of the results, we were able to achieve our goal of producing nanostructured for a-C:N.

The a-C:N, on the other hand, was coated on the p-Si substrate to form the p-n junction as one of the promising materials for carbon-based solar cell applications. The a-C:N/p-Si layer was sandwiched between the top and bottom gold (Au; thickness 60nm) layers. The Au was used to provide an active area for the device with the configuration Au/a-C:N/p-Si/Au. The device displayed photovoltaic properties under AM 1.5 SUN light (100 mW/cm2, 25°C), as illustrated in fig.8. The equation $=(Voc)(Jsc)(FF)/(Jph)$ was used to calculate the overall efficiency, Jsc is short circuit current density, Voc is open circuit voltage, and Jph is incoming photon flux (Valentini et al., 2001). For all samples, the incident photon flux was confirmed to be 0%. The cell exhibits only a slightly rectifying curve in a dark environment, but the presence of the rectifying curve confirms the hetero-junction of the p-n junction. The p-n junction is critical for creating charge separation between light-induced electrons and holes. The efficiency was 0% in the dark, but climbed to 0.001648% for 650°C and 0.000124% for 600°C at AM 1.5 SUN conditions (100 mW/cm2, 25°C).

(a)
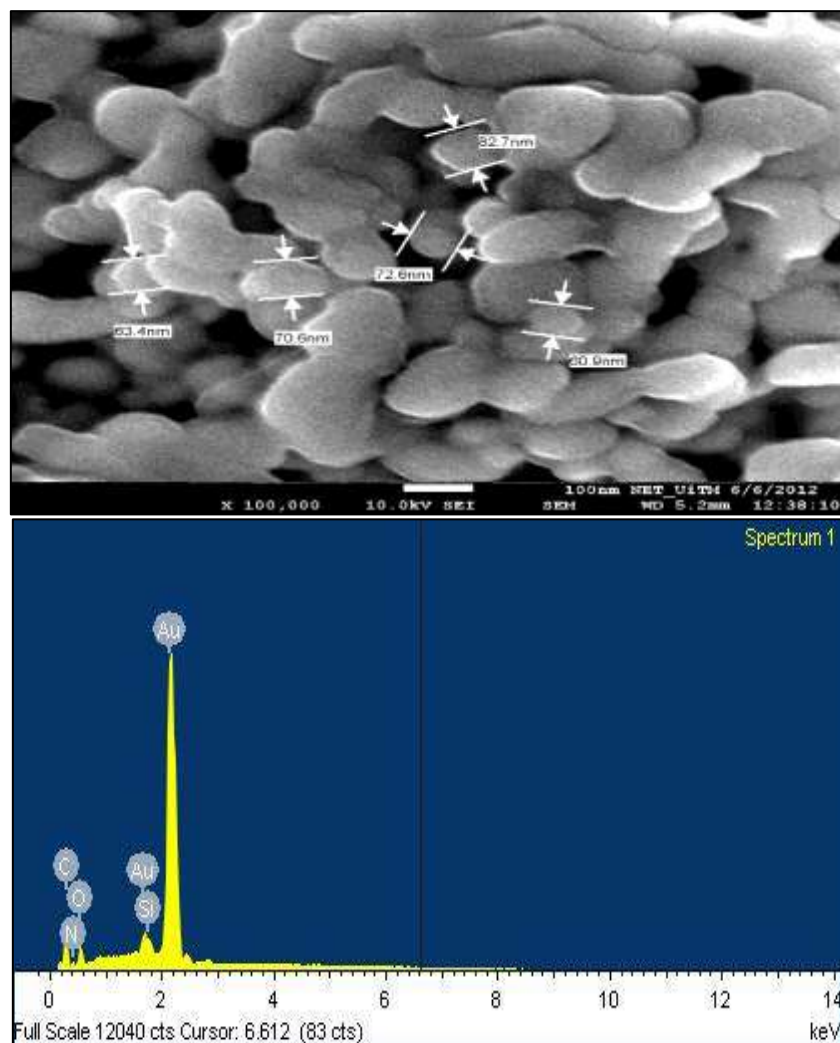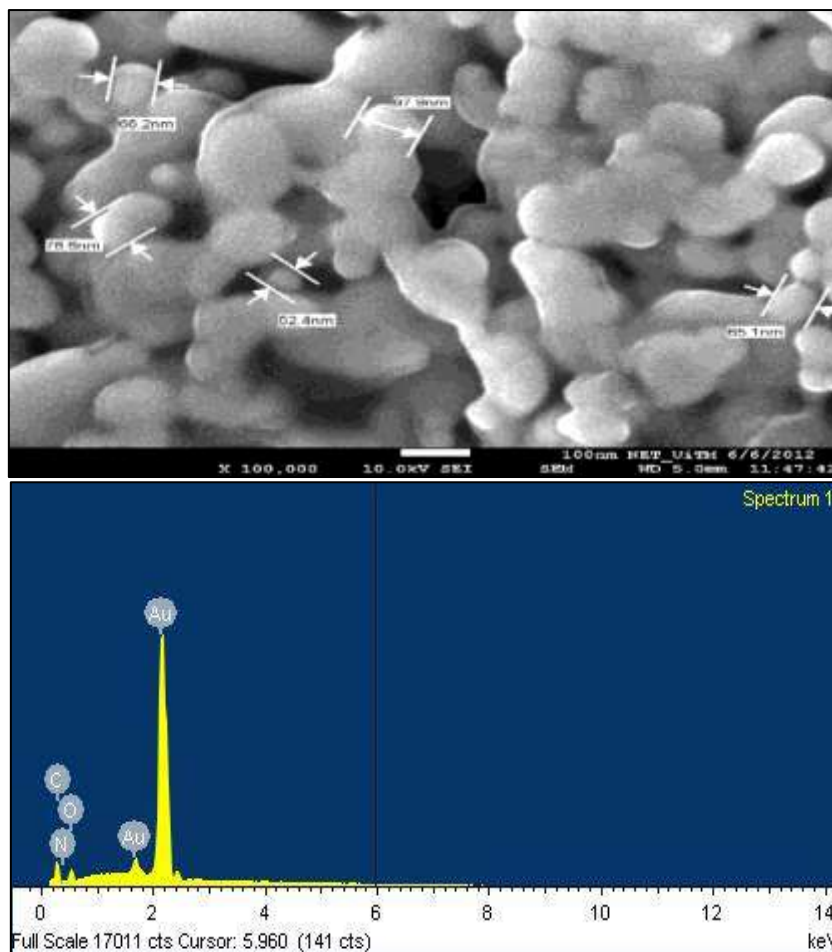
Fig.7. FESEM images and EDX spectrum for sample deposited at (a) 600°C and (b) 650°
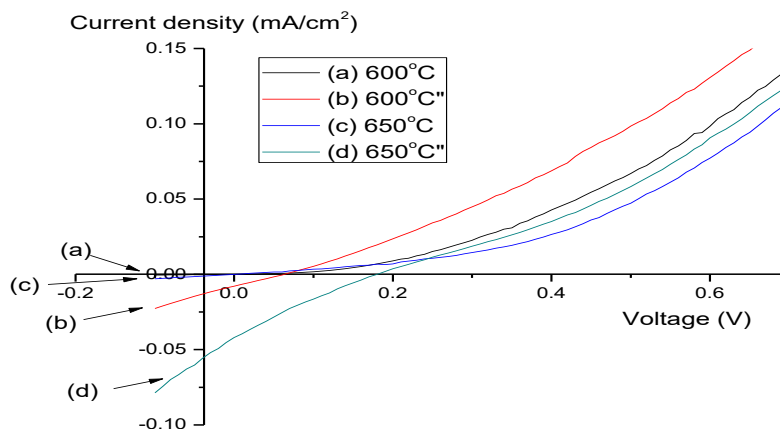

Fig.8. Current density-voltage (J-V) graph for sample deposited at 600°C and 650°C.
(" indicates illuminated sample under AM-1.5 illumination (100mW/cm²)

Conclusion
Finally, the nano-structured a-C thin films were created using the newly developed Aerosol-assisted CVD process and the natural precursor camphor oil. The electrical properties of the I-V solar simulator characterisation were examined, and an ohmic contact characteristic with

a high electrical conductivity value of 38 Scm-1 was obtained. The optical properties were evaluated using a UV-Vis-NIR Spectroscope with an absorption coefficient of 107 cm-1, and the optical band gap obtained was in the correct order for the a-C, which are 0.2 eV and 0.8 eV, respectively. The surface morphology of the a-C:N, on the other hand, was studied using FESEM and EDX. The appearance of the a-C:N was recognised using FESEM images, and the grain size was calculated. The grain size was determined to be in the nano-scale range of 4080nm (less than 100nm). The EDX characterisation indicates successful N doping in the a-C, as evidenced by the existence of the N peak. Finally, the suitability of the a-C:N to create the p-n junction with the p-Si substrate was explored as one of the promising materials for carbon-based solar cell applications. The successful formation of a hetero-junction between the p and n layers resulted in rectifying curves with efficiencies of 0.001648% for 650°C and 0.000124% for 600°C.

Motivation

Low-cost solar cell fabrication technologies are motivated by a variety of factors, all of which aim to make solar energy more accessible, economical, and pervasive. Affordable Renewable Energy, Energy Access in Developing Regions, Mass Production and Economies of Scale, Deployment and Market Growth, and Sustainability and Environmental Impact are some of the primary motivations.

Acknowledgement

References

Adhikari, S., Aryal, H. R., Ghimire, D. C., Kalita, G., & Umeno, M. (2008). Optical band gap of nitrogenated amorphous carbon thin films synthesized by microwave surface wave plasma CVD. *Diamond and Related Materials*, *17*(7–10), 1666–1668. https://doi.org/10.1016/J.DIAMOND.2008.03.027

Adhikari, S., Ghimire, D. C., Aryal, H. R., Adhikary, S., Uchida, H., & Umeno, M. (2006). Boron-doped hydrogenated amorphous carbon films grown by surface-wave mode microwave plasma chemical vapor deposition. *Diamond and Related Materials*, *15*(11–12), 1909–1912. https://doi.org/10.1016/J.DIAMOND.2006.07.022

Belaidi, A., Bayon, R., Dloczik, L., Ernst, K., Lux-Steiner, M. C., & Konenkamp, R. (2003). Comparison of different thin film absorbers used in eta-solar cells. *Thin Solid Films*, *431–432*, 488–491. https://doi.org/10.1016/S0040-6090(03)00223-2

Hauser, J. J. (1977). Electrical, structural and optical properties of amorphous carbon. *Journal of Non-Crystalline Solids*, *23*(1), 21–41. https://doi.org/10.1016/0022-3093(77)90035-7

Hou, X., & Choy, K. L. (2006). Processing and Applications of Aerosol-Assisted Chemical Vapor Deposition. *Chemical Vapor Deposition*, *12*(10), 583–596. https://doi.org/10.1002/CVDE.200600033

Huang, L. Y., & Meng, L. (2007). Effects of film thickness on microstructure and electrical properties of the pyrite films. *Materials Science and Engineering: B*, *137*(1–3), 310–314. https://doi.org/10.1016/J.MSEB.2006.11.029

Liu, A., Wu, H., Zhu, J., Han, J., & Niu, L. (2008). Evolution of compressive stress and electrical conductivity of tetrahedral amorphous carbon films with phosphorus incorporation. *Diamond and Related Materials*, *17*(11), 1927–1932. https://doi.org/10.1016/J.DIAMOND.2008.04.008

Liu, S., Wang, G., & Wang, Z. (2007). Study of the conductivity of nitrogen doped tetrahedral amorphous carbon films. *Journal of Non-Crystalline Solids*, *353*(29), 2796–2798. https://doi.org/10.1016/J.JNONCRYSOL.2007.05.021

Nolan, M. G., Hamilton, J. A., Obrien, S., Bruno, G., Pereira, L., Fortunato, E., Martins, R., Povey, I. M., & Pemble, M. E. (2011). The characterisation of aerosol assisted CVD conducting, photocatalytic indium doped zinc oxide films. *Journal of Photochemistry and Photobiology A: Chemistry*, *219*(1), 10–15. https://doi.org/10.1016/J.JPHOTOCHEM.2011.01.010

Omer, A. M. M., Rusop, M., Adhikari, S., Adhikary, S., Uchida, H., & Umeno, M. (2005). Photovoltaic characteristics of nitrogen-doped amorphous carbon thin-films grown on quartz and flexible plastic substrates by microwave surface wave plasma CVD. *Diamond and Related Materials*, *14*(3–7), 1084–1088. https://doi.org/10.1016/J.DIAMOND.2004.12.010

Robertson, J. (2002a). Diamond-like amorphous carbon. *Materials Science and Engineering: R: Reports*, *37*(4–6), 129–281. https://doi.org/10.1016/S0927-796X(02)00005-0

Robertson, J. (2002b). Diamond-like amorphous carbon. *Materials Science and Engineering: R: Reports*, *37*(4–6), 129–281. https://doi.org/10.1016/S0927-796X(02)00005-0

Robertson, J., & Davis, C. A. (1995). Nitrogen doping of tetrahedral amorphous carbon. *Diamond and Related Materials*, *4*(4), 441–444. https://doi.org/10.1016/0925-9635(94)05265-4

Rusop, M., Adhikari, S., Omer, A. M. M., Soga, T., Jimbo, T., & Umeno, M. (2006). Effects of methane gas flow rate on the optoelectrical properties of nitrogenated carbon thin films grown by surface wave microwave plasma chemical vapor deposition. *Diamond and Related Materials*, *15*(2–3), 371–377. https://doi.org/10.1016/J.DIAMOND.2005.07.034

Singh, R. S., Rangari, V. K., Sanagapalli, S., Jayaraman, V., Mahendra, S., & Singh, V. P. (2004). Nano-structured CdTe, CdS and TiO2 for thin film solar cell applications. *Solar Energy Materials and Solar Cells*, *82*(1–2), 315–330. https://doi.org/10.1016/J.SOLMAT.2004.02.006

Sitch, P. K., Jungnickel, G., Köhler, T., Frauenheim, T., & Porezag, D. (1998). p- and n-Type doping in carbon modifications. *Journal of Non-Crystalline Solids*, *227–230*(PART 1), 607–611. https://doi.org/10.1016/S0022-3093(98)00232-4

Suemasu, T., Saito, T., Toh, K., Okada, A., & Khan, M. A. (2011). Photoresponse properties of BaSi2 epitaxial films grown on the tunnel junction for high-efficiency thin-film solar cells. *Thin Solid Films*, *519*(24), 8501–8504. https://doi.org/10.1016/J.TSF.2011.05.028

Valentini, L., Kenny, J. M., Gerbig, Y., Savan, A., Haefke, H., Lozzi, L., & Santucci, S. (2001). Structure and mechanical properties of argon assisted carbon nitride films. *Thin Solid Films*, *398–399*(399), 124–129. https://doi.org/10.1016/S0040-6090(01)01458-4

Yap, S. S., Yow, H. K., & Tou, T. Y. (2009). Amorphous carbon–silicon heterojunctions by pulsed Nd:YAG laser deposition. *Thin Solid Films*, *517*(18), 5569–5572. https://doi.org/10.1016/J.TSF.2009.02.144

Zeng, A., Yin, Y., Bilek, M., & McKenzie, D. (2005). Ohmic contact to nitrogen doped amorphous carbon films. *Surface and Coatings Technology*, *198*(1–3), 202–205. https://doi.org/10.1016/J.SURFCOAT.2004.10.038